



# S1PR1 predicts patient survival and promotes chemotherapy drug resistance in gastric cancer cells through STAT3 constitutive activation

Shiyu Song<sup>a</sup>, Haiyan Min<sup>a</sup>, Mengyuan Niu<sup>a</sup>, Lei Wang<sup>a</sup>, Yongzheng Wu<sup>a</sup>, Bin Zhang<sup>b</sup>, Xiufang Chen<sup>c</sup>, Qiao Liang<sup>a</sup>, Yanting Wen<sup>a</sup>, Yong Wang<sup>a</sup>, Long Yi<sup>a</sup>, Hongwei Wang<sup>a,\*</sup>, Qian Gao<sup>a,\*</sup>

<sup>a</sup> Center for Translational Medicine and Jiangsu Key Laboratory of Molecular Medicine, Medical School of Nanjing University, Nanjing 210093, Jiangsu Province, China

<sup>b</sup> Central Laboratory, Nanjing Chest Hospital, Medical School of Southeast University, Nanjing 210029, Jiangsu Province, China

<sup>c</sup> Department of Biochemistry, School of Basic Medical Sciences, Wenzhou Medical University, Wenzhou 325035, Zhejiang Province, China

## ARTICLE INFO

### Article history:

Received 11 July 2018

Received in revised form 28 September 2018

Accepted 1 October 2018

Available online 10 October 2018

## ABSTRACT

**Background:** S1PR1-STAT3 inter-regulatory loop was initially suggested to be oncogenic in several cancer cells. However, the clinical relevance of this mechanism in tumor progression, disease prognosis and drug response was not established.

**Methods:** The correlations between S1PR1 transcription, overall survival and chemotherapy response of GC patients were tested using a large clinical database. The relevance of S1PR1 expression and STAT3 activation in both tumor tissues and cancer cell lines was also tested. The effect of S1PR1 high expression achieved by persistent STAT3 activation on tumor cell drug resistance was investigated *in vitro* and *in vivo*.

**Findings:** An enhanced S1PR1 expression was highly related with a reduced overall survival time and a worse response to chemotherapy drug and closer correlation to STAT3 in gastric cancer patients. The issue chip analysis showed that the expressions of S1PR1 and STAT3 activation were increased in higher graded gastric cancer (GC) tissues. Cellular studies supported the notion that the high S1PR1 expression was responsible for drug resistance in GC cells through a molecular pattern derived by constitutive activation of STAT3. The disruption of S1PR1-STAT3 signaling significantly re-sensitized drug resistance in GC cells *in vitro* and *in vivo*.

**Interpretation:** S1PR1-STAT3 signaling may participate drug resistance in GC, thus could serve as a drug target to increase the efficacy of GC treatment.

**Fund:** This work was supported by the National Natural Science Foundation of China (No. 81570775, 81471095), the grant from the research projects in traditional Chinese medicine industry of China (No. 201507004-2).

© 2018 The Authors. Published by Elsevier B.V. This is an open access article under the CC BY-NC-ND license (<http://creativecommons.org/licenses/by-nc-nd/4.0/>).

## 1. Introduction

Sphingosine-1-phosphate receptor (S1PR1), also known as endothelial differentiation gene 1 (EDG1), is a G-protein-coupled receptor mediating the bioactivity of signaling molecule sphingosine 1-phosphate (S1P) that promotes cell proliferation and survival [1,2]. More recently, it is suggested that a positive regulatory interaction with signal transducer and activator of transcription 3 (STAT3) is involved in tumorigenesis [3–6]. However, this effect of S1PR1 was mainly obtained upon ectopic expressions in cancer cells. The clinical relevance of S1PR1 in tumorigenesis and prognosis remains to be established. Specifically, the role of S1PR1 in human solid cancers, such as GC, was not yet determined.

Multiple drug resistance (MDR) is the autonomous adaptation of cancer cells to chemotherapy drugs over tumor growth and/or drug treatment in various cancers, including breast, ovarian, lung, and gastrointestinal tract cancers [7]. Numerous mechanisms, such as drug uptake/efflux, DNA repair and anti-apoptosis were involved in the adaptation [7–9]. The heterogeneity in genetics, signaling pathways and/or metabolic patterns in different tumor cells greatly influenced the sensitivity to chemotherapies [10,11]. A stratification of the diseases upon their molecular/cellular characteristics, as well as tissue origins to guide the treatment is much desired.

Previously, we found that a constitutive activation of Signal transducer and activator of transcription 3 (STAT3) in human GC cells significantly facilitated cellular drug resistance through multiple processes, including enhancing the expressions of oncogenes and vacuolar ATPase pump, and downregulating apoptotic molecules, implicating itself as an important indicator of MDR [12]. STAT3 is a key transcription factor that mediates the expressions of a variety of genes in response to cell stimuli

\* Corresponding authors.

E-mail addresses: [hwang@nju.edu.cn](mailto:hwang@nju.edu.cn) (H. Wang), [qian\\_gao@nju.edu.cn](mailto:qian_gao@nju.edu.cn) (Q. Gao).

## Research in context

### Evidence before this study

Gastric cancer (GC) is one of the most common cancers worldwide. Chemotherapy remains the primary treatment for GCs. However, the responses of the GC patients to chemotherapy were often unpredictable and the proportion of the patients with unfavorable prognoses remains high.

Multiple drug resistance (MDR) is the autonomous adaptation of cancer cells to chemotherapy drugs. Previously, we found that a constitutive activation of STAT3 in human GC cells significantly facilitated cellular drug resistance through multiple processes, implicating itself as an important indicator of MDR. S1PR1 is suggested to form a positive regulatory interaction with STAT3 in tumorigenesis. However, this effect of S1PR1 was mainly obtained upon ectopic expressions in cancer cells. The clinical relevance of S1PR1 in tumorigenesis and prognosis was not established. Specifically, the role of S1PR1 in human solid cancers, such as GC, was not yet determined.

### Added value of this study

We showed that an enhanced S1PR1 expression was highly related with a reduced overall survival time in gastric cancer patients. Moreover, the patients with a worse response to chemotherapy showed a higher S1PR1 levels and closer correlation to STAT3. And the expression of S1PR1 was correlated phosphorylated STAT3, its activated form, in higher graded GC tissues. The over expression S1PR1 was responsible for drug resistance in GC cells through a molecular pattern derived by a constitutive activation of STAT3. The disruption of S1PR1-STAT3 signaling significantly re-sensitized the drug resistant GC cells *in vitro* and *in vivo*.

### Implications of all the available evidence

The present work indicates that S1PR1 pathway is correlated with a significant reduction of survival time and worse chemotherapy response in GC patients. And S1PR1 inhibitor FTY720 reversed GC cells chemotherapy resistance partly. Thus, S1PR1-STAT3 axis may be a promising molecular target for GC treatment.

and plays a key role in cell survival [13–15]. It also initiates inflammation, programmed death-ligand 1 (PD-L1) upregulation and cell transformation in numerous malignant cells, and underlays bad prognosis of the diseases [16,17].

Herein, we presented data to show that an increased expression of S1PR1 was highly related to drug resistance in GC cells and worse outcome in clinical GC patients. Moreover, enhanced S1PR1 expression was co-localized with persistent STAT3 phosphorylation in clinical GC samples, in particular, in high graded ones. The disruption of S1PR1 signaling by FTY720 (Fingolimod), a clinically approved S1PR1 antagonist, proved effective in suppressing STAT3 activation and re-sensitizing drug resistant tumor cells to chemo treatment *in vitro* and *in vivo*.

## 2. Materials and methods

### 2.1. Reagents and antibodies

FTY720 was purchased from Cayman Chemical Company (Ann Arbor, MI, USA). Cisplatin (DDP) was purchased from Qilu Pharm (Shandong, China). Rabbit anti STAT3 and phosphor-STAT3 (Tyr705,

PY-STAT3) and mouse anti phosphor-STAT3 (Tyr705, PY-STAT3) antibodies were purchased from Cell Signaling Technology (Boston, MA, USA). Rabbit monoclonal antibodies against S1PR1, Mcl-1, Bcl-xl, Survivin and GAPDH were purchased from Abcam (Cambridge, MA, USA). Alexa Fluor 594 conjugated Donkey Anti-Mouse IgG (H + L) Antibodies, Alexa Fluor 488 conjugated Donkey Anti-Rabbit IgG (H + L) Antibodies, and Annexin V-FITC/PI double staining Apoptosis Detection Kit were purchased from Life technology (New York, NY, USA). BCA Protein Assay Kit was purchased from Pierce (Rockford, IL, USA).

### 2.2. Cell culture and cell transfection

The human gastric cell line BGC803, BGC823, MGC803, HGC27, MKN45, SGC7901 and the drug resistant cell line SGC7901/DDP were purchased from China Center for Type Culture Collection and distributed by Keygen biotech (Jiangsu, China). The cells were cultured in RPMI 1640 (Life technology, New York, NY, USA) supplemented with 10% fetal bovine serum (Hyclone, Logan, UT, USA), 100 units/mL penicillin and 100 mg/mL streptomycin (Hyclone, Logan, UT, USA), in humidified 5% CO<sub>2</sub> at 37 °C. Drug Resistant cancer cell line SGC7901/DDP was cultured in the same medium containing 2 μM of DDP. The siRNA oligo for S1PR1, 5'-ACAAGCACUAUACCUUU-3', for STAT3, 5'-CCCGUCAACAAUUUAGAA-3', scrambled control 5'-UUCUCCGAACGUGACACGUUU-3', were synthesized by Life technology (New York, NY, USA). For RNA interference, 100 pmol for 6-well plate or 5 pmol for 96-well plate S1PR1 siRNA was transfected by lipofectamine RNAiMAX reagent (Life technology, New York, NY, USA), the transfection was performed following the manufacturer's instruction. 24 h after transfection, the cells were treated with indicated drug for 24 h before analysis. The ORF of S1PR1 was cloned to pCDNA3.1 plasmid and transfected to tumor cells by lipofectamin 3000 reagent (Life technology, New York, NY, USA), after transfection for 24 h, the cells were treated with DDP.

### 2.3. Cell viability and apoptosis assay

Cells were seeded at a density of  $1 \times 10^5$  cells/mL in 96 well plates with four replications, and starved for 24 h without serum before drug challenge. Cell viability assays were performed using the CellTiter 96 AQueous One Solution Cell Proliferation Assay kit (Promega, Madison, WI, USA) after treatment with 2 fold diluted DDP for 24 h. The absorbance at 490 nm was measured using a microplate reader (Biotech, Winoski, VT, USA). For apoptosis assays, cells cultured in 6 well plate were harvested and stained with AnnexinV-FITC and propidium iodide and assessed for the percentage of double-negative population using a Calibur flow cytometer (BD, Franklin lake, NJ, USA), and Apoptosis data were analyzed using FlowJo Version 7.6.2 software (TreeStar, USA).

### 2.4. Immunoblotting and ELISA

Cells and tissues were lysed by RIPA buffer on ice, and then the concentration of protein was detected by a BCA protein kit. 50 μg protein of each sample was resolved on 10% sodium dodecyl sulfate polyacrylamide gel electrophoresis, transferred to nitrocellulose membrane and detected by indicated antibodies.

### 2.5. Immunofluorescence

Immunostaining was performed as standard protocol. Briefly, the cells were fixed on glass slide in 10% neutral formalin solution in cold PBS. And the patients' samples were rehydrated and retrieved by Tris-EDTA solution (pH 9.0). After blockage with 10 FBS, the slides were incubated with rabbit anti human S1PR1 antibodies and mouse anti human pY-STAT3 with the dilution of 1/100 at 4 °C overnight and washed thrice in PBS. Alexa Fluor 488 donkey anti rabbit secondary antibodies and Alexa Fluor 594 donkey anti-mouse secondary antibody were added to detect the S1PR1 and pY-STAT3 expression. DAPI was

added to reveal the nuclear of the cells. Immunofluorescence was visualized in FV10i Laser Scanning Confocal Microscope (Olympus, Center Valley, PA, USA). And the colocalization value was analyzed by Coloc 2 method with Fiji Software.

## 2.6. Mouse xenograft assays

6-week male Nude Balb/c mice were obtained from Model Animal Research Center of Nanjing University, cultured in a SPF condition. Mouse care and *in vivo* experimental procedures was approved by the Institutional Animal Care and Use Committee of the Nanjing University. A cell suspension of SGC7901/DDP cell ( $2 \times 10^6$ ) in PBS was injected subcutaneously into nude mice's right flank region. About ten days after the injection, the tumor cells formed measurable tumor sphere. And then the mice were divided randomly into different groups ( $n = 10$ ), receiving different treatment. Tumor-bearing mice were treated with the combination of FTY720 (5 mg/kg) and DDP (3 mg/kg), low DDP (3 mg/kg), High DDP (7.5 mg/kg) and FTY720 (5 mg/kg) by intraperitoneal injection every 2 days. PBS and DMSO were injected as control. The volumes of the tumor were measured before each treatment. 21 days after the first treatment, mice were sacrificed and the tumor spheres were removed by surgery and weighted to evaluate the inhibition of the drug.

## 2.7. TUNEL assay

TUNEL assay was performed by ApoBrdU DNA Fragmentation Assay Kit (Biovision, San Francisco, CA, USA) following manufacturer's instruction. Briefly, the tumor sphere was removed from implanted region and fix with 4% paraformaldehyde and embedded in paraffin. And then remove paraffin by immersing slides in fresh xylene twice. After rehydration, the slides were fixed with 4% paraformaldehyde and washed. Proteinase K was added to remove the remained protein on the slide, then the slides were washed and incubated with DNA labeling solution. FITC labeled anti Brdu antibody was added after washes twice and then incubated the slides RT for 30 min. Then the slides were washed and PI was adopted to reveal the nuclear of the cells. And the images were captured by FV10i Laser Scanning Confocal Microscope (Olympus, Center Valley, PA, USA).

## 2.8. Real-time PCR

mRNA was extracted from cultured cells and tumor sphere using RNeasy Micro Kit (Qiagen, Hilden, Germany), Total mRNA was reversed transcribed into cDNA with PrimeScript RT Master mix (TaKaRa, Otsu, Japan). SYBR green quantitative real-time PCR was performed, using PCR Master Mix (Life technology, New York, NY, USA). The expression of target gene was determined relative to beta actin and relative expression was calculated by  $\Delta\Delta C_t$  method.

## 2.9. Immunohistochemistry-paraffin

Immunohistochemistry was performed by standard protocol. Briefly, the tumor sphere was removed from implanted region and fixed with 4% paraformaldehyde and embedded in paraffin. After hydrolysis and antigen retrieval, the slides of both tumor bearing mouse and human patients were blocked and washed with PBS. Immunostaining was carried out with rabbit monoclonal antibody to pY-STAT3, S1PR1, and Ki-67 at 4 °C overnight, respectively. And an UltraVision Quanto Detection System (Thermo, Waltham, MA, USA) was adopted to detect the expression level of indicated proteins. The Stages of gastric tumor cells were evaluated by pathologists. And the image was analyzed by Fiji Software [18]. Generally, the picture of each section was firstly color-separated by color deconvolution using the H-DAB method. The Optical density and the area of DAB staining of color-separated picture was calculated by adjusted threshold. The Immuno Score of each

sample was calculated by this equation:  $IS = \text{Log}(O \cdot A)$ , where IS means Immuno Score, O means the optical density and A means the total area of the DAB staining of each sample.

## 2.10. Clinical data preparation and analysis

TCGA (The Cancer Genome Atlas) data including gene expression data (level 3,  $N = 439$ ) and clinical information ( $N = 443$ ) were downloaded from the Cancer Genome Atlas (TCGA-STAD) web server through GDC-client software. The information of interest was then extracted, combined and/or normalized. The correlation was calculated by Spearman's correlation test for the data that was not normally distributed. The treatment outcome was defined by TCGA follow-up data of the patients who received chemotherapy. Only patients with full information of both drug usage and response were selected and calculated. The information about tumor stages on the tissue chips was provided by either the supplier (Zhuoli Biotech, Shanghai) or our collaborators at Taizhou hospital affiliated to Wenzhou Medical University.

## 2.11. Statistical analysis

For animal experiments, ten mice were assigned a pretreatment group. The size and weight of mice and tumors were compared using Student's *t*-test (for comparisons of two groups) and analysis of variance (for multiple group comparisons). For cell based assays, 3 independent replications were tested and calculated. For values that were not normally distributed (as determined by the Kolmogorov–Smirnov test), the Mann–Whitney's rank sum test was used. A *P*-value <0.05 was deemed statistically significant. All statistical tests were two-sided and were performed using Graphpad prism 6 (GraphPad Software, La Jolla, CA, USA).

## 3. Results

### 3.1. S1PR1 expression predicted overall survival time in gastric cancer patients

The transcript levels of S1PR1 and clinical outcome of gastric cancer patients was analyzed. As shown in Fig. 1A patients with gastric cancer who had a higher expression of S1PR1 in the tumor tissues exhibited a significantly shortened overall survival time comparing to that of low expression ones (median survival time 779 days in high vs. 1686 days in low). To explore this finding, we then validated the correlation of S1PR1 expression with survival time of different types of cancer patients available on <http://www.oncolnc.org/> [19]. Surprisingly, the result found in gastric cancer was not observed in either breast cancer, melanoma or lung cancer patients (Supplementary Fig. S1A), contradicting with a cell line based observation [20]. In addition, the transcript level of S1PR1 was significantly increased with the stage development of the cancers (Fig. 1A), so was the protein level (Fig. 1B, C) determined by a commercially available GC tissue. The immuno-score (IS) of S1PR1, which indexes both the % of positive staining cells and the density of the staining (see Methods), was markedly increased along the stage development of the tumors (Fig. 1D). Thus, the expression of S1PR1 in GC tissues were related to tumor progression.

To assess whether the clinical potency of S1PR1 was through STAT3, the correlation between S1PR1 and STAT3 was analyzed. Indeed, the transcription of S1PR1 was significantly correlated with STAT3 and STAT3 downstream gene SOCS3 in GC samples (Fig. 1D and Supplementary Fig. S1B). Similarly, the expression of S1PR1 proteins was also significantly correlating with the level of 705 Tyrosine phosphorylation of STAT3 (pY-STAT3), a direct measurement of STAT3 activation, in a paired gastric tissue chips (Fig. 1E, F; Supplementary Fig. S1C). To detect the co-localization of S1PR1 and pY-STAT3 in the same cancer cells, an immunofluorescent double staining of S1PR1 and pY-STAT3 in a home-made human GC tissue chip that included 59 gastric tissues with 36 later stage cancer biopsies (stage III or above) and 23 non-tumor gastric

tissues was performed. In this chip, 20 of 36 (55.6%) tumor samples showed co-localization of high levels of S1PR1 and pY-STAT3 in cancer cells (M1 > 80%), with the S1PR1 staining at more peripheral of the cells surrounding a central pY-STAT3 staining (Fig. 1G). No pY-STAT3 positive cells were detected in para-cancerous (n = 6) and normal gastric tissues (n = 17). These results suggested that an enhanced S1PR1 along with a persistent activation of STAT3 was common in high graded gastric cancers.

### 3.2. Hyper-expression of S1PR1 promoted drug resistance in gastric cancer cells

To determine the molecular function of high S1PR1 and persistent activation of STAT3 in gastric cancer, the levels of S1PR1 expression in a pair of related human GC cells, SGC7901 vs. SGC7901/DDP cells, with >4-folds differences in IC<sub>50</sub> value to DDP (14.08 ± 0.8766 μM vs. 3.149 ± 0.1837 μM, respectively, Supplementary Fig. S2A) were compared. We previously found that a persistent STAT3 activation was drug resistance-causing with the activations of multiple mechanisms [12]. Notably, an elevated S1PR1 expression was detected in SGC7901/DDP cells, but not in its parental drug sensitive SGC7901 cells (Fig. 2A). In addition to an increase of STAT3 phosphorylation in the SGC7901/DDP cells, the levels of STAT3 downstream gene Mcl-1, Bcl-xl and Survivin that are known to promote tumor cells survival [21] were also upregulated at both transcript and protein levels (Fig. 2A,B). Immunofluorescent assay revealed the co-localization of S1PR1 and PY-STAT3 in SGC7901/DDP cells (Fig. 2C). Thus, the high S1PR1 in GC cells functioned as a facilitator of MDR is likely through STAT3 activation.

To determine whether the correlation between drug resistance and high expression of S1PR1 was common in GC cells, 5 more frequently used human GC cell lines were studied. 2 of 5 cell lines, HGC27 and MKN45, showed a drug resistance phenotype, as well as higher S1PR1 expression (Fig. 2D and Supplementary Fig. S2B). In these cells, upregulation of STAT3 phosphorylation and expressions of STAT3 downstream gene Mcl-1, Bcl-xl and Survivin were also observed (Fig. 2E). Thus, drug resistant gastric cancer cells exhibited hyper-expressions of S1PR1 and increased STAT3-related cell survival signaling, which was consistent with the fact that progressive disease (PD) patients presented a higher S1PR1 level and closer correlation with STAT3 than complete remission/response (CR) patients who received chemotherapy (Fig. 2F and Supplementary Fig. S2C, D).

### 3.3. Mutual regulations between S1PR1 and STAT3 underlay drug resistance in GC cells

To relate S1PR1 expression and STAT3 activation in human GC cells, SGC7901/DDP cells were treated with S1P, its natural lipid ligand of S1PR1. A significant increase of STAT3 phosphorylation accompanied with an upregulation of STAT3 downstream survival genes and S1PR1 was detected (Fig. 3A). In addition, overexpression of S1PR1 gene in drug sensitive SGC7901 cells upregulated STAT3 phosphorylation and the expressions of its downstream genes (Fig. 3B), and induced drug resistance (Fig. 3C). In contrast, S1PR1 knocking down in SGC7901/DDP cells downregulated STAT3 phosphorylation and the expressions of its target genes (Fig. 3D), significantly sensitized otherwise drug resistant cells to DDP, resulting higher levels of apoptosis (Fig. 3E, F). On the other hand, STAT3 knocking down in SGC7901/DDP cells reduced the expression of S1PR1 (Fig. 3G) and abolished the pro-survival effect of S1P, suggesting S1PR1 related drug resistance depended on STAT3 activation (Fig. 3H).

### 3.4. S1PR1 was a sensitive target for restoring drug sensitivity in human GC cells

To explore whether S1PR1 is a sensitive target for drug resistance in human GC cells. The S1PR1 antagonist FTY720 that was clinically

approved for multiple sclerosis was tested. As shown in Fig. 4A, B, while FTY720 (10 μM) treatment exhibited largely reduced STAT3 phosphorylation and its downstream pro-survival genes at both protein and mRNA levels in SGC7901/DDP cells. However, it showed no detective effects on direct cell killing in both SGC7901 and SGC7901/DDP cells (Supplementary Fig. S3A). However, the supplement of FTY720 for 12 h prior to DDP treatment shown a strong synergistic effect on SGC7901/DDP cell killing (Fig. 4C). It enhanced the killing power of DDP on SGC7901/DDP cells at a low DDP concentration (2.5 μM) that otherwise is well tolerated by these cells (Fig. 4D, E). In contrast, this synergistic effect between DDP and FTY720 was not observed in drug sensitive SGC7901 cells, presumably due to the lack of S1PR1-STAT3 pathway in these cells (Supplementary Fig. S3B). Consistently, treatment of FTY720 in drug resistant HGC27 and MKN45 cells also downregulated the transcript and protein levels of STAT3 downstream genes and S1PR1 (Supplementary Fig. S3C, D), and greatly enhanced the apoptosis, when supplemented before DDP challenge (Supplementary Fig. S3F).

To determine whether this FTY720 effect on DDP resistant cells was significant *in vivo*, an engrafted tumor mouse model was established by implanted the SGC7901/DDP cells subcutaneously in nude mice. The mice (n = 10) that received a low dose DDP (3 mg/kg) showed no significant effect on reducing tumor size, as compared to that of controls (n = 10). However, the mice that received same amount of DDP in combined with FTY720 (5 mg/kg) resulted in a significant inhibition of tumor growth. And administration of FTY720 (5 mg/kg) alone partially blocked tumor growth in the testing animals (Fig. 5A, B). Furthermore, the combinatory treatment exhibited a comparable killing power at the high dose DDP (7.5 mg/kg), but avoided its severe toxic effect that was shown by a sharp body weight loss in testing animals (Supplementary Fig. S4A, B) and 2 of total 10 high dose DDP treated mice died at day 14 and 18.

As expected, at molecular level, the expressions of STAT3 downstream genes were significantly lower in response to FTY720 treatment (Fig. 5C). Importantly, FTY720 significantly downregulated the expression of S1PR1, so did STAT3 phosphorylation in the engrafted tumor tissues (Fig. 5D). TUNEL assay revealed that the combination of FTY720 and DDP resulted a massive apoptosis in the tumor sections (Fig. 5E). Immunohistochemistry showed significantly reduced pY-STAT3 and S1PR1 staining in the deep regions of tumor tissues. The cell proliferation mark Ki67 that was highly expressed in the engrafted tumor cells was also significantly inhibited upon the combination of FTY720 treatment (Supplementary Fig. S4C). Thus, blockage of S1PR1 signaling by FTY720 was effective in sensitizing drug resistant GC cells to DDP and enhanced drug-caused cell death with less toxicity in solid GC animal model.

## 4. Discussion

Chemotherapy is still the first-line clinical choice for the treatment of various cancers. Precisely predicting high response and low toxic solutions are urgently needed. MDR, among numerous mechanisms that affect the outcomes of chemotherapy, is the major cell autonomous adaptations directly contributed to the insensitivity of tumor cells to chemotherapy drugs. However, the mechanism underlying MDR was not well defined and remained largely unclear. Previously, in human gastric cancer cells, we found that a constitutively activated STAT3 is essential in maintaining drug resistance in cells involving multiple cellular processes, and the disruption of STAT3 re-sensitized the cells to DDP, indicating that an ectopic activation of STAT3 may led to, at least in some scenarios, MDR [12]. However, how this ill-triggered and maintained STAT3 activation was achieved in these cells was not known, which limited one to develop methods for tumor cell specific STAT3 disruption, whereas directly targeting STAT3 has its disadvantages and lack of efficacy and specificity *in vivo* [22]. Moreover, from epidemiological point of view, whether STAT3-related MDR is clinically significant was not known.

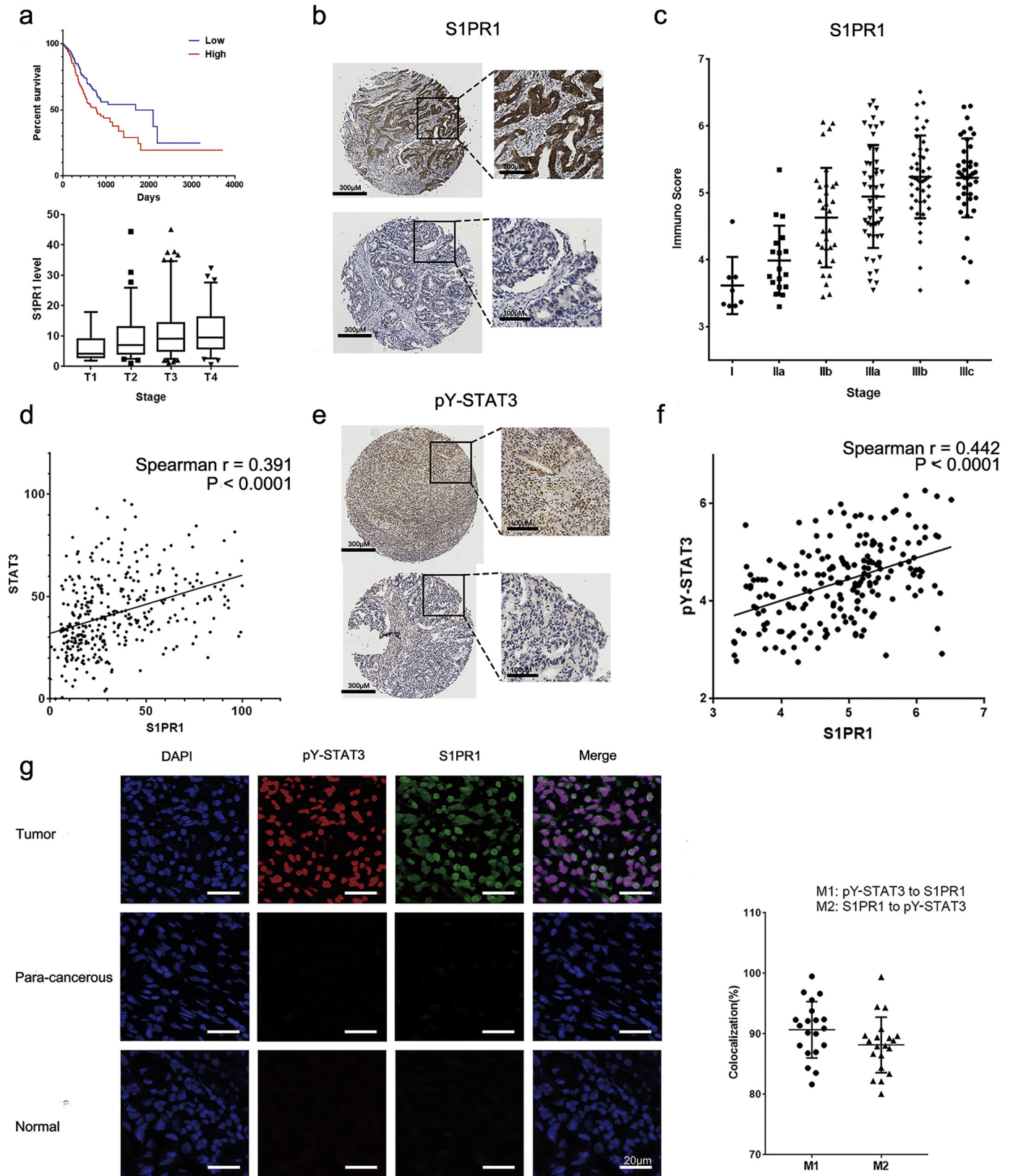


**Fig. 1.** S1PR1 and pY-STAT3 were highly expressed in gastric cancer patients. (A) upper panel, Kaplan-Meier plots for overall survival of high and low transcript levels of S1PR1 in gastric cancer patients; lower panel transcript levels of S1PR1 in 4 stages of gastric cancer patients. (B) Immunohistochemistry staining of S1PR1 of gastric cancer patient tissues. Upper panel: a stage IIIb sample, lower panel: a stage IIa sample. Scale bar: 200 µM left panel, 100 µM right panel. (C) Immuno score levels of S1PR1 in different stage of gastric cancer patients were compared. (D) Correlation of S1PR1 and STAT3 transcript levels in gastric cancer patients. (E) Immunohistochemistry staining of pY-STAT3 of gastric cancer patient tissues. Upper panel stage IIIc, lower panel stage IIa. Scale bar: 200 µM left panel, 100 µM right panel. (F) Correlation of S1PR1 and pY-STAT3 protein levels determined by IS in gastric cancer patients. (G) Left panel: Immunofluorescence double staining of S1PR1 (green) and pY-STAT3 (red) in gastric tumor, para-cancerous and normal samples, DAPI (blue) was adopted to reveal the nuclear of the cells. Scale bar: 20 µM. Right panel, quantification of patient tissue sections for percentages of overlapping red (pY-STAT3) and green (S1PR1) channels, shown as Manders colocalization coefficients M1 (p-STAT3 to S1PR1) and M2 (S1PR1 to p-STAT3), respectively.

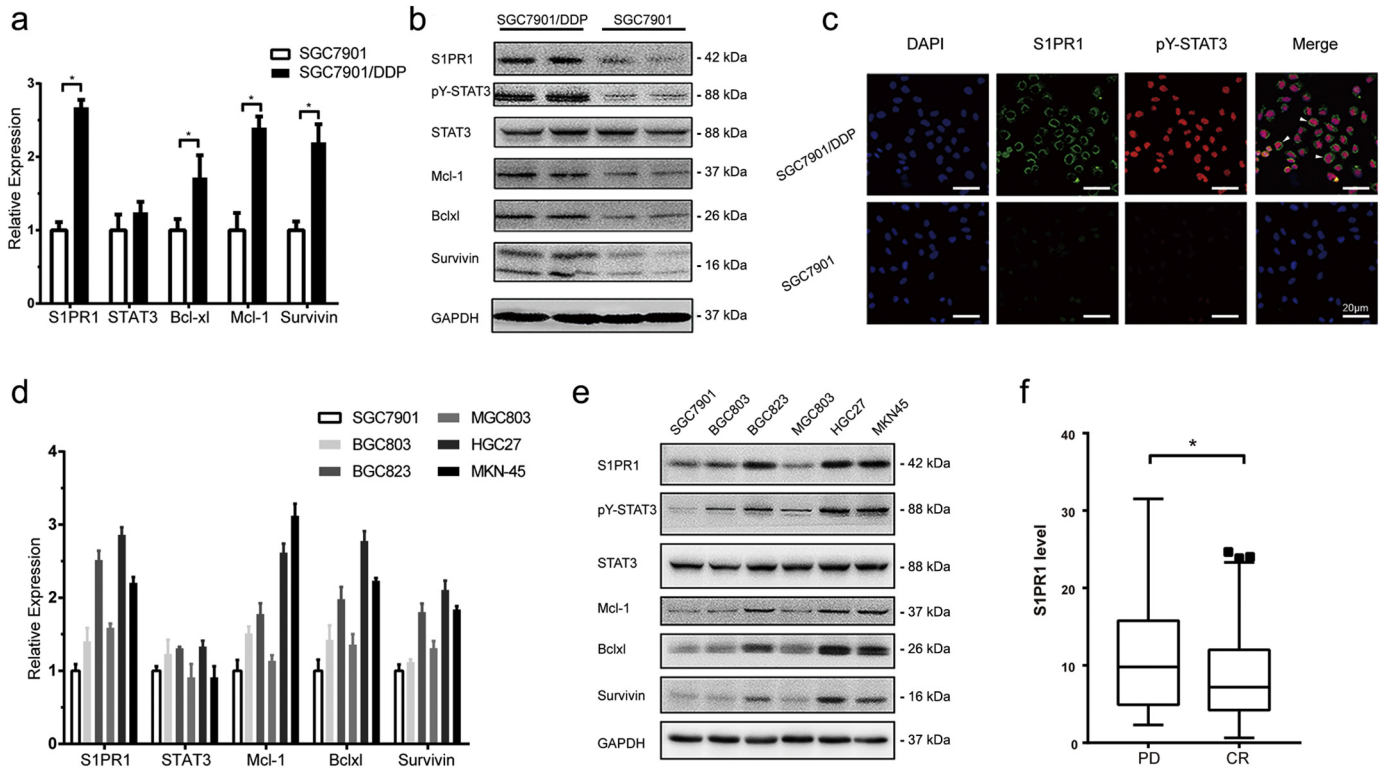


**Fig. 2.** Hyper expression of S1PR1 in gastric cancer cells identified drug resistance. (A) Transcript levels determined by QPCR and (B) protein expression levels determined by Western blot of indicated genes of SGC7901 and SGC7901/DDP gastric cancer cell lines. Data were expressed as mean  $\pm$  SD,  $n = 5$ . \* $P < 0.05$  (Student's  $t$ -test). (C) Immunofluorescence double staining of S1PR1 (green) and pY-STAT3 (red) in SGC7901 and SGC7901/DDP cells. White arrow indicated the colocalization of each protein. DAPI (blue) was adopted to reveal the nuclear of the cells. Scale bar: 20  $\mu$ m. (D) Transcript levels and (E) protein expression levels of indicated genes of different gastric tumor cell lines were detected by QPCR or Western blot, respectively. Data were expressed as mean  $\pm$  SD,  $n = 5$ . (F) Transcript levels of S1PR1 in gastric cancer patients who were reported to receive chemotherapy drug in TCGA database. The patients were divided into two groups of PD (progressive disease) and CR (complete remission/response) according to the follow up report.

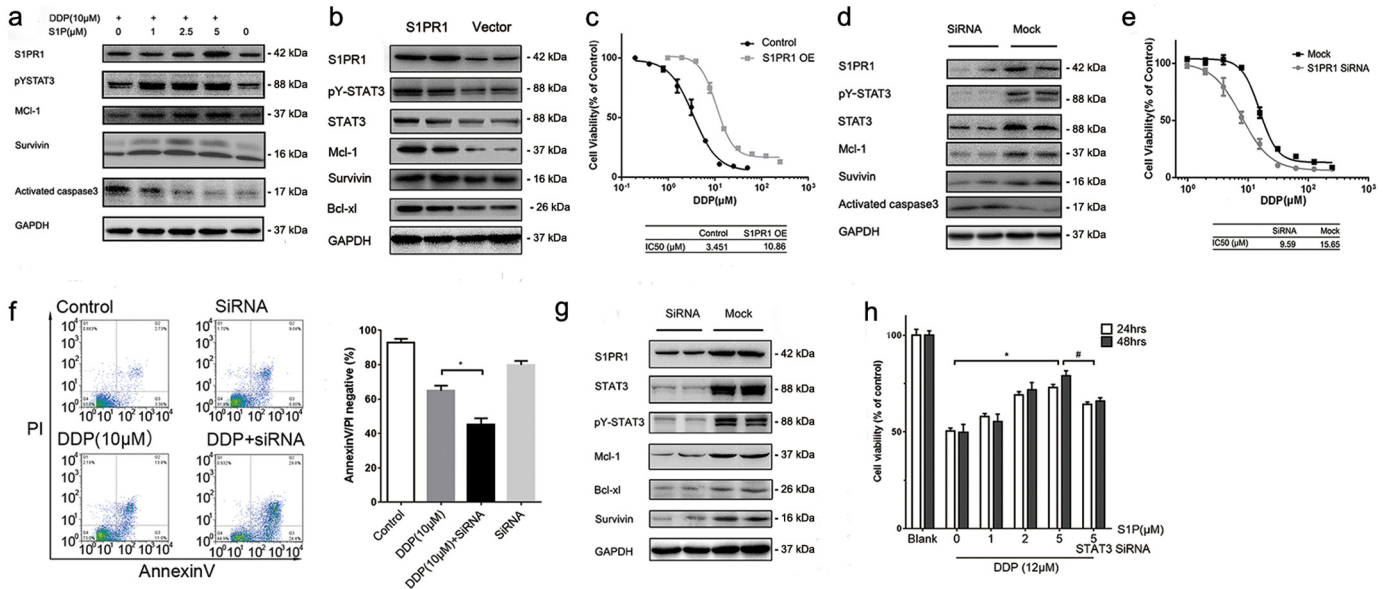


**Fig. 3.** S1PR1-STAT3 formed a positive regulatory loop in GC cells and contributed to drug resistance. (A) Expression of indicated genes of SGC7901/DDP cells after treated with different concentrations of S1P and DDP for 24 h was detected by Western blot. (B) Expression of indicated genes of SGC7901 cells transfected with S1PR1 over-expression and empty vectors for 48 h was detected by Western blot. (C) SGC7901 cells transfected with S1PR1 overexpression or empty vector cells were treated with fold diluted DDP for 24 h and the cell viability was detected by MTS method. Data were expressed as mean  $\pm$  SD,  $n = 4$ . (D) Expression of indicated genes of SGC7901/DDP cells transfected with S1PR1 siRNA and mock siRNA for 48 h was determined by Western blot. (E) Cell viability of SGC7901/DDP cells, tested by MTS method. Cells were treated with fold diluted DDP for 24 h with or without S1PR1 knocking down. Data were expressed as mean  $\pm$  SD,  $n = 4$ . (F) Cell apoptosis levels of SGC7901/DDP cells were determined by AnnexinV/PI double staining with FACS after indicated treatment for 24 h. The ratio of double negative population of the cells was presented with mean  $\pm$  SD,  $n = 5$ . \* $P < 0.05$  (Student's  $t$ -test). (G) Expression of indicated genes of SGC7901/DDP cells transfected with STAT3 siRNA and mock siRNA was detected by Western blot. (H) Cell viability of SGC7901/DDP cells treated with fold diluted DDP for 24 or 48 h after transfection of S1PR1 and mock siRNA was detected by MTS. Data were expressed as mean  $\pm$  SD,  $n = 4$ . \* $P < 0.05$ , # $P < 0.05$  (Student's  $t$ -test)

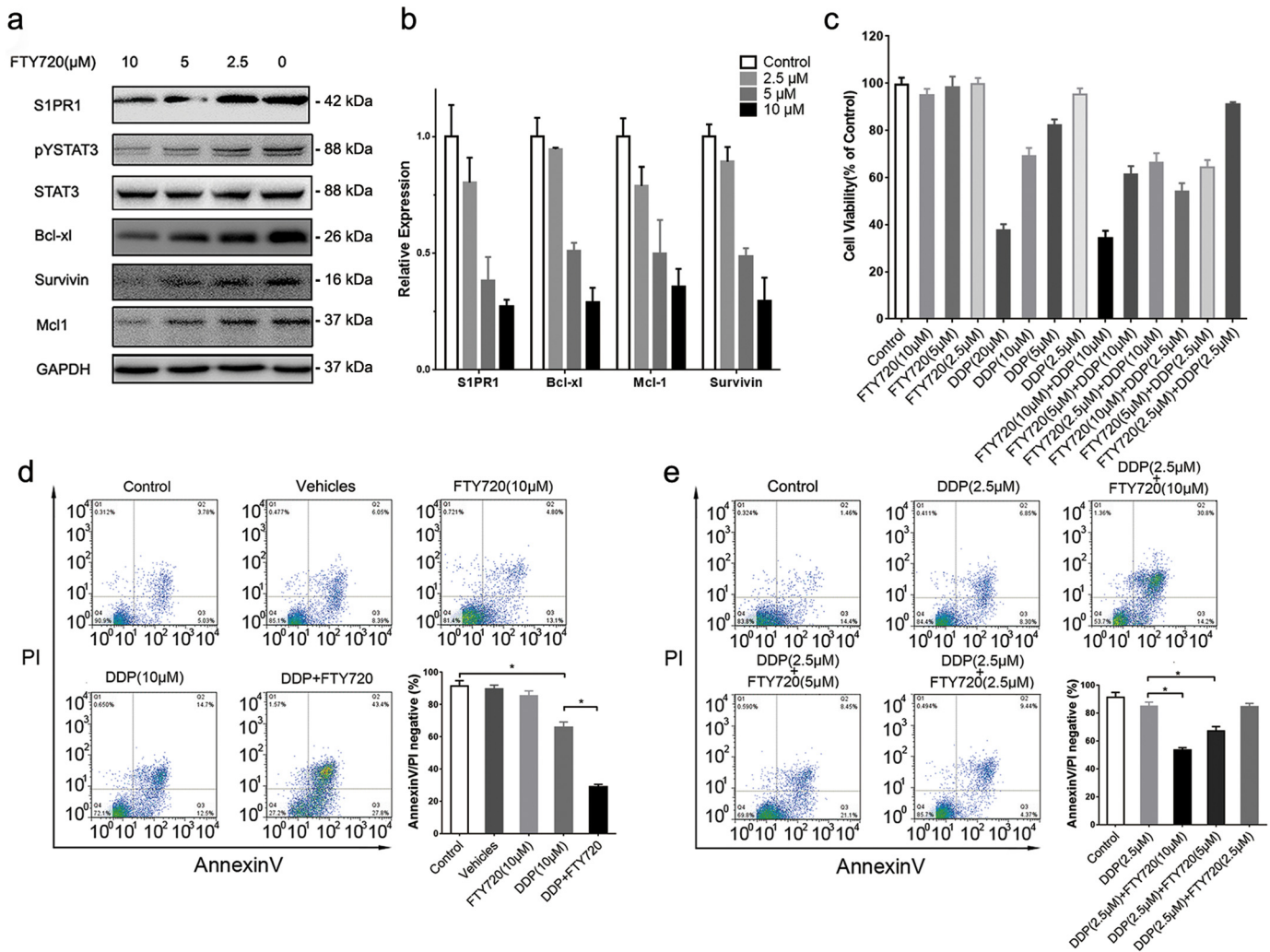


**Fig. 4.** FTY720 restored drug sensitivity in human GC cells *in vitro*. (A) Expression of indicated genes of SGC7901/DDP cells treated with different concentration of FTY720 for 24 h was detected by Western blot. (B) Transcript levels of indicated genes of SGC7901/DDP cells after treatment of FTY720 for 24 h were determined by QPCR. Data were expressed as mean  $\pm$  SD,  $n = 5$ . (C) Cell viability of SGC7901/DDP cells was detected by MTS. The cancer cells were treated with indicated combination of FTY720 and DDP for 24 h. Data were expressed as mean  $\pm$  SD,  $n = 4$ . (D and E) Cell apoptosis levels of SGC7901/DDP cells with indicated treatment, were determined by AnnexinV/PI double staining with FACS. The ratio of double negative population of the cells was presented with mean  $\pm$  SD,  $n = 5$ . \* $P < 0.05$  (Student's *t*-test).

In conclusion, we used clinical observations to argue the relevance of S1PR1-STAT3 in MDR in GCs. We showed that an increased expression of S1PR1 at transcript level in the tumor tissues predicted a significant reduction of survival time in gastric cancer patients. Tissue array studies uncovered that the high expression of S1PR1 proteins that co-localized with pY-STAT3 was common in higher graded GC tissues. Cell studies confirmed S1PR1-STAT3 positive feedback loop that conferred the drug resistance in human GC cells. Consistently, the patients with a worse response to chemotherapy drugs showed a higher S1PR1 expression and closer correlation to STAT3.

FTY720, a clinically approved first-line immunosuppressive drug, also known as fingolimod, is a S1PR1 antagonist initially synthesized to simplify the complex structure of myriocin (ISP-1), a fungal metabolite with immunosuppressive properties isolated from *Isaria sinclairii* [23]. Because of its structural analog with sphingosine, FTY720 is capable of inhibiting lymphocyte migration from lymphoid organs through S1PR1 binding [23,24]. More recently, FTY720 was found to be effective in the treatment of a rodent B cell lymphoma model through its disruptive function on S1PR1-STAT3 feedback loop [4]. Moreover, FTY720 was suggested to influence neural cell migration and function through S1PR1 [25] and act as a HDAC inhibitor or PP2A activator. It has been

reported to have a beneficial effect on cancer cell killing in a S1PR1 independent manner [26,27]. These possible side effects of FTY720 indicated the need for careful measurement while exploring the clinical application of FTY720 in cancer drug resistance.

The FTY720 dose (5 mg/kg/every other day) adopted in our experiment was about 2.5 times higher when compared to that of clinical does, maximum 5 mg/person daily, after a cross-species adjustment [28]. However, we did not observe any obvious toxicities measured by body weight, food intake, general behavior and histopathological examinations of the livers, kidneys, spleens and lungs (data not shown), applied either FTY 720 alone or combined with DDP (2.5 mg/kg). Moreover, an immune-safety was also observed in a monkey study with an extreme high-dose (10 mg/kg/day) and a long-lasting treatment (52 days), suggesting a general safety of the drug [29].

Importantly, in this study, we showed a specific blockage of S1PR1-STAT3 signaling by FTY720 that re-sensitized drug resistance in human GC cells with a significant down-regulation of the expression of S1PR1 and STAT3 activation. FTY720 caused no direct induction of cell death in drug resistant cells, however, a synergy effect of FTY720 and DDP was strong both *in vitro* and *in vivo*. Thus, FTY720 may be a

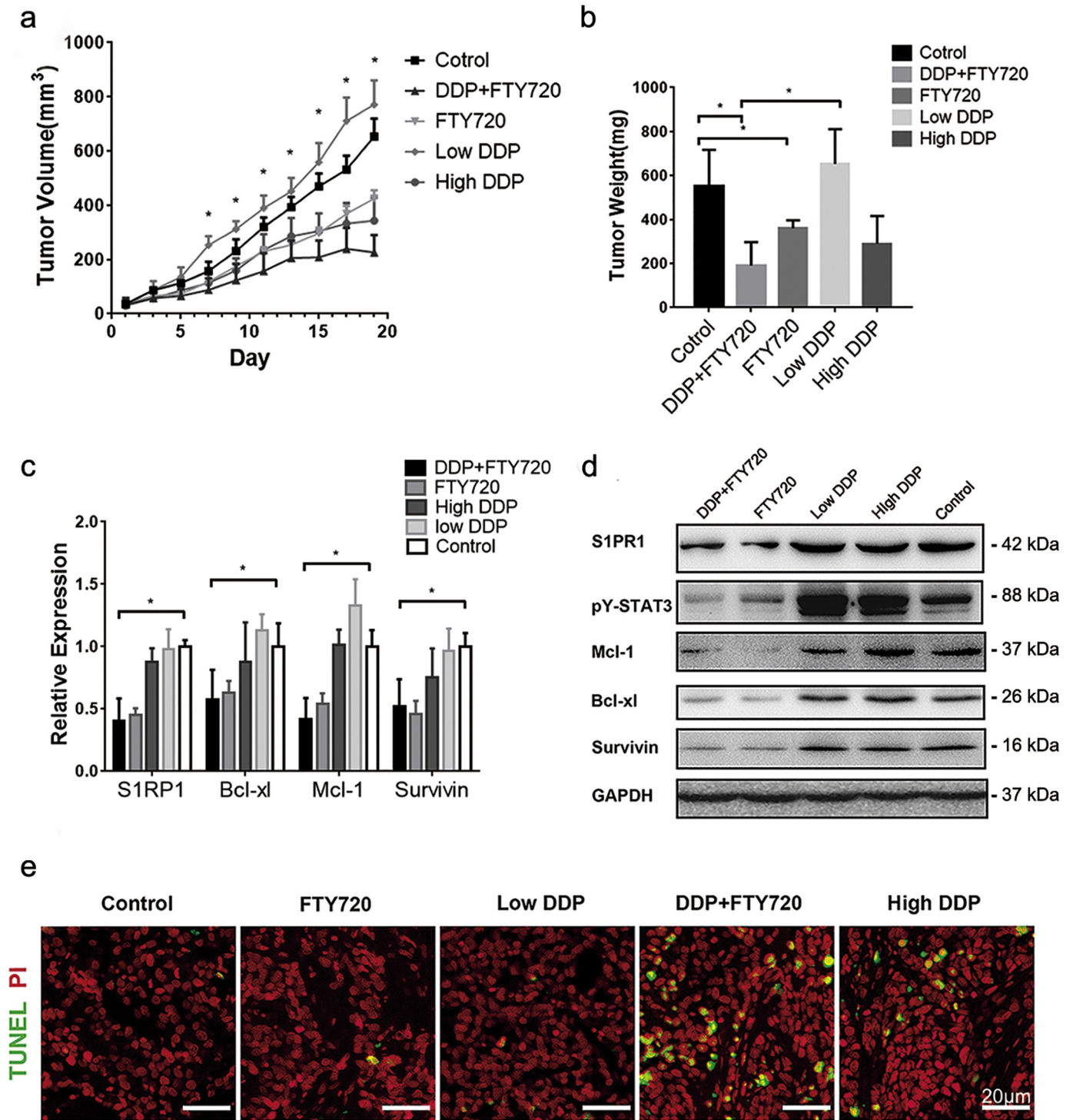


**Fig. 5.** FTY720 and DDP have a strong synergistic effect in human GC cells *in vivo*. (A) Tumor volume of mice implanted with SGC7901/DDP receiving indicated treatment every other day, measured before drug injection. Data was presented with mean  $\pm$  SD, n = 10. \*P < 0.05 (Student's *t*-test) of FTY720 + DDP group comparing with control group. (B) The tumors removed from the mice were weighted at the end of the experiment. The tumor weight was presented with mean  $\pm$  SD, n = 10. \*P < 0.05 (Student's *t*-test). (C) Transcript levels and (D) expression levels of indicated genes in SGC7901/DDP tumor sphere were determined by QPCR or Western blot, data were expressed as mean  $\pm$  SD, n = 10. \*P < 0.05 (Student's *t*-test). (E) Cell apoptosis in tumor tissue of each group was determined by TUNEL staining. Scale bar: 20  $\mu$ m.

potent candidate for improving the efficiency of chemotherapy in drug resistant GCs.

Supplementary data to this article can be found online at <https://doi.org/10.1016/j.ebiom.2018.10.005>.

#### Conflict of interest

The authors declare no conflict of interest.



## Acknowledgements

This work was supported by the National Natural Science Foundation of China (No. 81570775, 81471095), the grant from the research projects in traditional Chinese medicine industry of China (No. 201507004-2.).

## Author contributions statement

The authors contributed in the following way: S-SY, M-HY, N-MY: performed most of the experiments. S-SY, W-HW, GQ wrote the manuscript; WL and W-YZ: performed the plasmid construction and infection; ZB, C-XF, LQ: prepared the reagents; W-YT: performed the western blotting; WY, YL performed the immunohistochemical scoring; S-SY, N-MY: performed data analysis; W-YT, C-XF edited and revised the manuscript; S-SY, W-HW, GQ: designed the study, revised the manuscript, and provided administrative management. All authors have read and approved the final manuscript.

## References

- [1] Spiegel S, Milstien S. The outs and the ins of sphingosine-1-phosphate in immunity. *Nat Rev Immunol* 2011;11(6):403–15.
- [2] Liu YJ, Wada R, Yamashita T, Mi YD, Deng CX, Hobson JP, et al. Edg-1, the G protein-coupled receptor for sphingosine-1-phosphate, is essential for vascular maturation. *J Clin Invest* 2000;106(8):951–61.
- [3] Visentin B, Vekich JA, Sibbald BJ, Cavalli AL, Moreno KM, Matteo RG, et al. Validation of an anti-sphingosine-1-phosphate antibody as a potential therapeutic in reducing growth, invasion, and angiogenesis in multiple tumor lineages. *Cancer Cell* 2006;9(3):225–38.
- [4] Liu Y, Deng J, Wang L, Lee H, Armstrong B, Scuto A, et al. S1PR1 is an effective target to block STAT3 signaling in activated B cell-like diffuse large B-cell lymphoma. *Blood* 2012;120(7):1458–65.
- [5] Deng J, Liu Y, Lee H, Herrmann A, Zhang W, Zhang C, et al. S1PR1-STAT3 signaling is crucial for myeloid cell colonization at future metastatic sites. *Cancer Cell* 2012;21(5):642–54.
- [6] Pyne NJ, Pyne S. Sphingosine 1-phosphate is a missing link between chronic inflammation and colon cancer. *Cancer Cell* 2013;23(1):5–7.
- [7] Galluzzi L, Senovilla L, Vitale I, Michels J, Martins I, Kepp O, et al. Molecular mechanisms of cisplatin resistance. *Oncogene* 2012;31(15):1869–83.
- [8] Gottesman MM, Fojo T, Bates SE. Multidrug resistance in cancer: Role of ATP-dependent transporters. *Nat Rev Cancer* 2002;2(1):48–58.
- [9] Kelland L. The resurgence of platinum-based cancer chemotherapy. *Nat Rev Cancer* 2007;7(8):573–84.
- [10] Shi Y, Du L, Lin L, Wang Y. Tumour-associated mesenchymal stem/stromal cells: Emerging therapeutic targets. *Nat Rev Drug Discov* 2017;16(1):35–52.
- [11] Patch A, Christie EL, Etemadmoghadam D, Garsed DW, George J, Fereday S, et al. Whole-genome characterization of chemoresistant ovarian cancer. *Nature* 2015;521(7553):489–94.
- [12] Huang S, Chen M, Shen Y, Shen W, Guo H, Gao Q, et al. Inhibition of activated Stat3 reverses drug resistance to chemotherapeutic agents in gastric cancer cells. *Cancer Lett* 2012;315(2):198–205.
- [13] Levy DE, Lee CK. What does Stat3 do? *J Clin Invest* 2002;109(9):1143–8.
- [14] Lee H, Zhuang G, Cao Y, Du P, Kim H, Settleman J. Drug resistance via feedback activation of Stat3 in oncogene-addicted cancer cells. *Cancer Cell* 2014;26(2):207–21.
- [15] Bollrath J, Pheesse TJ, von Burstin VA, Putoczki T, Bennecke M, Bateman T, et al. gp130-mediated Stat3 activation in enterocytes regulates cell survival and cell-cycle progression during colitis-associated tumorigenesis. *Cancer Cell* 2009;15(2):91–102.
- [16] Yu H, Pardoll D, Jove R. STATs in cancer inflammation and immunity: A leading role for STAT3. *Nat Rev Cancer* 2009;9(11):798–809.
- [17] Chen J, Jiang CC, Jin L, Zhang XD. Regulation of PD-L1: A novel role of pro-survival signalling in cancer. *Ann Oncol* 2016;27(3):409–16.
- [18] Schindelin J, Arganda-Carrera I, Frise E, Kaynig V, Longair M, Pietzsch T, et al. Fiji: An open-source platform for biological-image analysis. *Nat Methods* 2012;9(7):676–82.
- [19] Anaya J, Juan H. OncoLnc: Linking TCGA survival data to mRNAs, miRNAs, and lncRNAs. *Peer J Comp Sci* 2016;2:e67.
- [20] Lee H, Deng J, Kujawski M, Yang C, Liu Y, Herrmann A, et al. STAT3-induced S1PR1 expression is crucial for persistent STAT3 activation in tumors. *Nat Med* 2010;16(12):1421–8.
- [21] Kamran MZ, Patil P, Gude RP. Role of STAT3 in cancer metastasis and translational advances. *Biomed Res Int* 2013;421821.
- [22] Miklosy G, Hilliard TS, Turkson J. Therapeutic modulators of STAT signalling for human diseases. *Nat Rev Drug Discov* 2013;12(8):611–29.
- [23] Brinkmann V, Pinschewer DD, Feng L, Chen S. FTY720: Altered lymphocyte traffic results in allograft protection. *Transplantation* 2001;72(7):764–9.
- [24] Brinkmann V, Davis MD, Heise CE, Albert R, Cottens S, Hof R, et al. The immune modulator FTY720 targets sphingosine 1-phosphate receptors. *J Biol Chem* 2002;277(24):21453–7.
- [25] Chun J, Hartung H. Mechanism of action of oral fingolimod (FTY720) in multiple sclerosis. *Clin Neuropharmacol* 2010;2(33):91–101.
- [26] Hait NC, Avni D, Yamada A, Nagahashi M, Aoyagi T, Aoki H, et al. The phosphorylated prodrug FTY720 is a histone deacetylase inhibitor that reactivates ER alpha expression and enhances hormonal therapy for breast cancer. *Oncogene* 2015;4:e156.
- [27] Saddoughi SA, Gencer S, Peterson YK, Ward KE, Mukhopadhyay A, Oaks J, et al. Sphingosine analogue drug FTY720 targets I2PP2A/SET and mediates lung tumour suppression via activation of PP2A-RIPK1-dependent necroptosis. *EMBO Mol Med* 2013;1(5):105–21.
- [28] Nair A, Jacob S. A simple practice guide for dose conversion between animals and human. *J Basic Clin Pharm* 2016;7(2):27.
- [29] Brinkmann V, Chen S, Feng L, Pinschewer D, Nikolova Z, Hof R. FTY720 alters lymphocyte homing and protects allografts without inducing general immunosuppression. *Transpl P* 2001;33(1–2):530–1.